

# Frequency-Domain Optical Coherence Tomography Assessment of Unprotected Left Main Coronary Artery Disease—A Comparison With Intravascular Ultrasound

Yusuke Fujino,<sup>1,2</sup> MD, Hiram G. Bezerra,<sup>1\*</sup> MD, PHD, Guilherme F. Attizzani,<sup>1</sup> MD, Wei Wang,<sup>1</sup> MS, Hirosada Yamamoto,<sup>1</sup> MD, Daniel Chamié,<sup>1</sup> MD, Tomoaki Kanaya,<sup>1</sup> MD, Emile Mehanna,<sup>1</sup> MD, Satoko Tahara,<sup>2</sup> MD, PHD, Sunao Nakamura,<sup>2</sup> MD, PHD, and Marco A. Costa,<sup>1</sup> MD, PHD

**Objectives:** To investigate safety and feasibility of imaging unprotected left main (ULM) using frequency-domain optical coherence tomography (FD-OCT) compared with intravascular ultrasound (IVUS). **Background:** IVUS has been used to assess and guide percutaneous coronary intervention (PCI) of ULM disease. FD-OCT offers 10-fold higher axial resolution than IVUS and its high-speed image acquisition obviates the need for proximal balloon occlusion. **Methods:** We prospectively enrolled 35 consecutive patients with ULM disease. FD-OCT and IVUS assessments were attempted pre- and post-PCI and compared in regards to safety, ability to image the region of interest (ROI), number of pullbacks, volume of contrast and ability to detect malapposition, dissection, and thrombus. **Results:** Patients were followed for 1 year when FD-OCT imaging was repeated. FD-OCT required more repeated pullbacks to image the ROI compared to IVUS. Mean lumen and stent areas were similar between FD-OCT and IVUS ( $11.24 \pm 2.66$  vs.  $10.85 \pm 2.47$  mm<sup>2</sup>,  $P = 0.13$  and  $10.44 \pm 2.33$  vs.  $10.49 \pm 2.32$  mm<sup>2</sup>,  $P = 0.82$ , respectively), whereas imaged stent length was shorter with FD-OCT. Malapposition areas and volumes were larger and more edge dissections were detected by FD-OCT. There were no clinical adverse events and no complications associated with FD-OCT at baseline and 1-year follow-up. All dissections were healed, whereas stent malapposition was still detected at follow-up. **Conclusions:** FD-OCT assessment of ULM is feasible and safe. Direct comparisons with IVUS reveal that FD-OCT achieved imaging completeness less often, whereas it was more sensitive in detecting malapposition and edge dissections, and similar to IVUS in the assessment of lumen and stent dimensions. © 2013 Wiley Periodicals, Inc.

**Key words:** optical coherence tomography; intravascular ultrasound; left main coronary artery disease; percutaneous coronary intervention

## INTRODUCTION

Percutaneous coronary intervention (PCI) of unprotected left main (ULM) coronary artery disease has gained significant adoption over the past decade [1,2]. This mode of therapy, however,

demands high procedural precision, given the large amount of myocardium at risk and often difficult to assess dimensions of ULM. The efficacy of intravascular imaging utilizing catheter-based ultrasound (IVUS) systems during PCI was reported previously

<sup>1</sup>Harrington Heart and Vascular Institute, University Hospitals Case Medical Center, Case Western Reserve University, Cleveland, Ohio

<sup>2</sup>Department of Cardiology, New Tokyo Hospital, Chiba, Japan

Conflict of interest: Nothing to report.

\*Correspondence to: Hiram G. Bezerra, MD, PhD, Assistant Professor of Medicine, Case Western Reserve University, Harrington Heart and Vascular Institute, University Hospitals Case Medical

Center, Case Western Reserve University, 11100 Euclid Avenue, Cleveland, OH 44106, Tel.: (216) 983-5887, Fax: (216) 844-8318. E-mail: hiram.bezerra@uhhospitals.org

Received 9 April 2012; Revision accepted 21 January 2013

DOI: 10.1002/ccd.24843

Published online 16 March 2013 in Wiley Online Library (wileyonlinelibrary.com).

[3,4] and has made significant contributions to our current understanding and treatment of ULM disease [5].

The possibility of imaging the ULM using a high-resolution imaging modality such as optical coherence tomography (OCT) is attractive. However, the first generation time-domain OCT systems had a relatively narrow field of view and required proximal vessel occlusion for image acquisition, precluding its application in ULM. Conversely, the new frequency-domain optical coherence tomography (FD-OCT) technology allows pullback speeds up to 25 mm/sec, which obviates the need for proximal vessel occlusion. FD-OCT also offers a larger (10 mm) field of view, enabling visualization of large vessels such as the ULM [6]. The role of OCT guiding PCI has been recently demonstrated by our group and others [7–9]. Therefore, we hypothesized that FD-OCT is a feasible and safe imaging modality to assess and guide therapy of ULM disease. The aims of this study were (1) to evaluate the performance of FD-OCT compared with IVUS during ULM PCI and (2) to investigate the safety and feasibility of repeat FD-OCT 1 year after ULM stenting.

## METHODS

### Study Design, Patient Selection, and Follow-up

From February 2010 to August 2010, 47 consecutive patients with ULM disease underwent PCI at New Tokyo Hospital (Chiba, Japan). Patients with stable angina or nonstent thrombosis (ST)-elevation myocardial infarction (MI) were eligible if they had >50% lesion stenosis of ULM by angiographic assessment. Stable angina patients should have documented ischemia. We defined unstable angina as having a progressive crescendo pattern or angina at rest without an increase in troponin levels. Non-ST-elevation MI was defined as having typical rise and gradual fall of troponin or creatine kinase myocardial band of myocardial necrosis with ischemic symptoms and development of pathologic Q-waves or ST segment depression on the electrocardiogram. The exclusion criteria included congestive heart failure with left ventricle ejection fraction of <30%, acute MI with ST-segment elevation, chronic kidney disease (serum creatinine, >1.5 mg/dL) not on dialysis, known allergy to antiplatelet agents or contrast dye, and life expectancy <1 year.

Both IVUS and FD-OCT were attempted in all patients with alternated order at pre- and post-PCI. By protocol, 1 year after PCI, patients with de novo lesions treated with a single drug-eluting stent underwent follow-up angiography and FD-OCT imaging. Clinical follow-up (office visit or phone call) was conducted at

1-year follow-up. The study protocol was approved by the institutional review board and informed consent was obtained for every patient before any intervention was performed.

### PCI Procedure

All patients were treated with aspirin (loading dose, 200 mg) and clopidogrel (loading dose, 300 mg) at least 24 hr before PCI. After stent implantation, aspirin was maintained indefinitely (200 mg/day), whereas clopidogrel (75 mg/day) was continued for at least 1 year. Cilostazol was also continued at least 3 months postprocedure [10]. All patients received an intra-arterial bolus injection of 6,000–10,000 IU of heparin and intracoronary isosorbide dinitrate (2–3 mg) before angiography. PCI was performed by femoral or radial approaches using 6 or 7F guiding catheters. IVUS and FD-OCT were attempted in all patients after intracoronary nitroglycerin infusion (100–200 µg). Sirolimus-eluting stents or everolimus-eluting stents were implanted as per the operator's discretion. PCI success was defined when <25% residual stenosis with normal distal blood flow (TIMI 3) was achieved.

### Quantitative Coronary Angiography Analysis

Quantitative coronary angiography (QCA) was performed pre- and post-PCI. Angiographic measurements were carried out in matched two orthogonal projections. Offline analyses of digital coronary angiograms were performed with (CASS II, Pie-Medical, Maastricht, The Netherlands) using validated quantitative methods [11].

### OCT Image Acquisition and Analysis

A conventional angioplasty guidewire (0.014 inch) was advanced distal to the region of interest (ROI), then the 2.7 French FD-OCT catheter (Dragonfly™, St. Jude Medical, St. Paul, MN) was advanced over the guidewire at least 10-mm distal to the ROI. The images were calibrated by automated adjustment of the Z-offset [6], and automated pullback was set at 20 mm/sec. Data were acquired using a commercially available FD-OCT system (C7-XR™, OCT Imaging System, St. Jude Medical, St. Paul, MN) and digitally stored. The injection of isosmolar contrast dye (100%) to displace blood was performed with a power injector. FD-OCT pullbacks were attempted from left anterior descending artery (LAD, 32/35 [91.4%]) or left circumflex artery (LCX, 3/35 [8.6%]) to the aorta-ostium. The acquisition of images after PCI was performed in a similar fashion. The amount of injected contrast as well as the settings utilized to acquire FD-OCT images/pullback was recorded. Total number of

pullbacks was recorded and the reasons for repeated pullbacks were classified as follows: insufficient blood clearance preventing good image acquisition, ROI longer than the FD-OCT maximum imaging length (54 mm), additional balloon angioplasty, and stent implantation. At 1-year follow-up, angiography and FD-OCT were repeated in a similar fashion. The images were analyzed by two independent investigators blinded to the angiographic and clinical data. FD-OCT analysis was performed using dedicated software with an automated contour-detection algorithm (Off-line Review Software, version C.0; St. Jude Medical, St. Paul, MN). FD-OCT assessments were performed offline and the information provided was not used to guide PCI in our study. All cross-sectional images were initially screened for quality assessment and excluded from analysis if any portion of the stent was out of the screen; if a side branch occupied  $>45^\circ$  of the cross-section; or if the image had poor quality caused by residual blood, artifact, or reverberation [6]. Two different regions were identified: the stented segment and the 5-mm distal to the stent. Image acquisition completeness was defined proximally when the left main ostium was visualized, and distally when the stented segment could be completely assessed. Pre-PCI images were analyzed every 1 mm, whereas post-PCI and follow-up FD-OCT images were analyzed every 0.4 mm. If suboptimal image quality was present, the analyst could select an adjacent frame at  $\pm 0.2$ -mm interval [12]. Quantitative measurements were performed and the presence of thrombus and dissections was determined as described previously [13,14]. Stent imaging completeness was defined when stent struts were observed in at least three quadrants at each segment. OCT-derived malapposition values were obtained by means of  $360^\circ$  chords, distributed between the lumen and the stent contours. Commercially available dedicated software (Amira 5.4.2, Visage Imaging, San Diego, CA) was used for three-dimensional reconstruction of FD-OCT two-dimensional images.

### IVUS Image Acquisition and Analysis

The Atlantis SR Pro 40 MHz catheter and the iLab ultrasound console (Boston Scientific, Natick, MA) were used for IVUS image acquisition. The catheter was advanced into the vessel, with the imaging device placed at least 10-mm distal to the ROI. Automated pullbacks were acquired at 1 mm/sec over the entire length of the ROI. All IVUS images were exported into DICOM standard format for subsequent offline analysis. Quantitative IVUS analysis was performed using a validated semi-automated detection algorithm (Curad, version 4.32, Wijk bij Duurstede, The Netherlands) by two independent experts as reported previously [15]. Semi-automatic lumen contour detection

was used for mean lumen area (MeanLA), minimal lumen area (MLA) in pre- (i.e., every 1-mm frame) and post-PCI (i.e., every 0.4-mm frame) assessments. Mean stent area (MeanSA) and minimal stent area (MSA) were obtained in post-PCI segments (every 0.4-mm frame). The presence of thrombus and dissections was determined. Malapposition was qualitatively defined by IVUS as regions containing blood speckle behind stent. Stent completeness was detected in a similar fashion as FD-OCT.

### Endpoints

The imaging methods were compared according to the following parameters [1]: safety endpoints including the occurrence of ST-segment changes during or after imaging acquisition, dissection associated with the guidewire, imaging catheters or contrast injection, arrhythmia, vessel occlusion, coronary spasm or slow flow assessed by thrombosis in myocardial infarction (TIMI) flow grade, and corrected TIMI frame count [16]. The occurrence of contrast-induced nephropathy (CIN), defined as a 25% increase (in absolute values of 0.5 mg/dL) of serum creatinine above baseline levels between 48 and 96 hr after the exposure to iodinated contrast dye [17], was also evaluated [2]; ability to image the ROI [3]; quality of image acquisition (visualized lesion and stent length), percentage of cross-sections out of the field of view [4], required number of pullbacks and volume of contrast [5], detection of malapposition, stent edge dissections and thrombus [6]; quantitative measurements (MeanLA, MLA, MeanSA, MSA, and malapposition area/volume).

The study also evaluated the safety and feasibility of repeated ULM FD-OCT imaging at 1 year after stent implantation. Baseline and follow-up FD-OCT parameters were compared. The occurrence of major cardiovascular cardiac events (cardiac death, acute MI, coronary artery bypass grafting [CABG], ST, and target lesion revascularization [TLR]) at 1 year follow-up after ULM PCI was recorded.

### Statistical Methods

The principal analysis was conducted using SAS 9.2 (SAS Institute, Cary, NC). Categorical variables are presented as number (proportion), and ordinal or continuous variables are presented as mean  $\pm$  SD. The difference between IVUS and OCT methodology was evaluated by paired *t*-test for continuous variables, and generalized estimating equations model for categorical variables. Bland–Altman plots were used to further evaluate lumen area measurements from IVUS and OCT modalities.

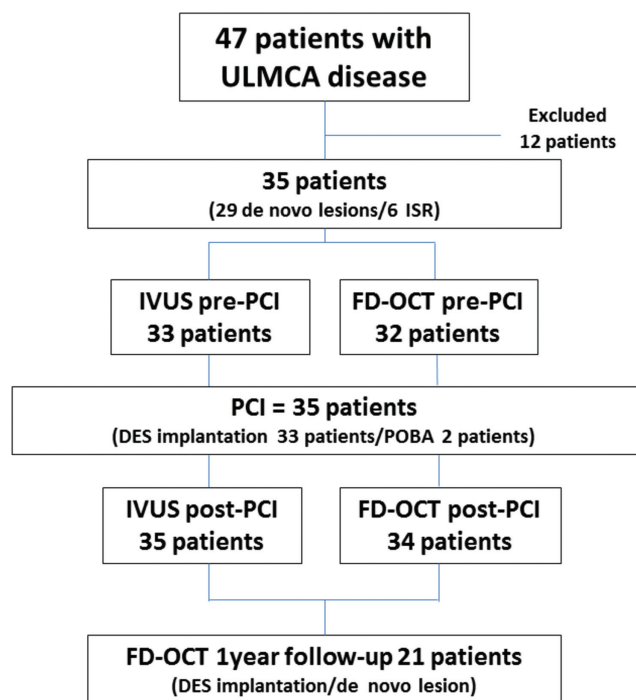


**Fig. 1.** Flow chart summarizing the patients, procedure, and image acquisitions included in this study. ULM: unprotected left main coronary artery, ISR: in-stent restenosis, IVUS: intravascular ultrasound, PCI: percutaneous coronary intervention, FD-OCT: frequency-domain optical coherence tomography, DES: drug-eluting stent, and POBA: plain old balloon angioplasty.

## RESULTS

Out of 47 patients, 12 were excluded as follows: five patients had baseline creatinine of  $>1.5$  mg/dL, two patients had ejection fraction of  $<30\%$ , one patient had protected left main disease, one patient was presented with ST-segment elevation MI, one patient had allergy to contrast dye, and two patients did not agree to sign the informed consent. Thirty-five patients fulfilled the inclusion criteria and were prospectively enrolled in the study (Fig. 1). Baseline characteristics of the study population are summarized in Table I. De novo lesions were presented in 29 patients and in-stent restenosis in six patients. There were seven patients (20%) with chronic kidney disease on hemodialysis. In nonhemodialysis patients, the average baseline creatinine level was  $0.82 \pm 0.23$  mg/dL. Table II summarizes the angiographic and procedural characteristics. One patient (2.9%) had ostial ULM disease and seven patients (20%) had true bifurcation lesions (Medina 1,1,1) [18]. Twenty-seven patients (77.1%) were treated with a single stent and six patients (17.1%) were treated with two stents. Two patients (5.7%) with in-stent restenosis were treated only with balloon

**TABLE I.** Baseline Clinical Characteristics<sup>a</sup>

	Patients (n = 35)
Age (years)	68.4 ± 7.8
Men, n (%)	30 (85.7)
BMI (kg/m <sup>2</sup> )	24.1 ± 3.9
Hypertension, n (%)	27 (77.1)
Diabetes, n (%)	15 (42.9)
HbA1c (%)	6.3 (1.6)
Dyslipidemia, n (%)	29 (82.9)
Current smoker, n (%)	10 (28.5)
Obesity, n (%)	15 (42.9)
Prior MI, n (%)	3 (8.6)
Prior CABG, n (%)	0 (0)
Post PCI, n (%)	17 (48.6)
Peripheral arterial disease, n (%)	5 (14.3)
Hemodialysis, n (%)	7 (20)
LV ejection fraction (%)	59.4 ± 8.2
Baseline creatinine non-HD (mg/dL)	0.82 ± 0.23
Baseline eGFR non-HD	72.6 ± 18.6
Congestive heart failure $< 30$ , n (%)	0 (0)
Stable angina, n (%)	29 (82.9)
Unstable angina, n (%)	6 (17.1)
Acute MI, n (%)	0 (0)
De novo, n (%)	29 (82.9)
ISR, n (%)	6 (17.1)

<sup>a</sup>Values are n (%) or mean ± SD.

Abbreviations: BMI: body mass index, MI: myocardial infarction, CABG: coronary artery bypass graft, PCI: percutaneous coronary intervention, LV: left ventricle, GFR: glomerular filtration rate, HD: hemodialysis, ISR: in-stent restenosis.

angioplasty (Table II). Inability to cross the stenosis precluded IVUS or FD-OCT imaging in two patients. FD-OCT could not cross one highly calcified plaque, which was successfully crossed by IVUS. The ability of IVUS and FD-OCT to acquire qualifying images was equivalent (100 vs. 96.9%, respectively,  $P = 0.313$ ). Changes in ST segment occurred in only one patient during imaging acquisition with both modalities. This patient had a calcified lesion with a high degree of stenosis (93% DS). All patients underwent IVUS images after PCI, whereas FD-OCT was deferred in one patient (2.9%) owing to concerns regarding amount of contrast dye already used during PCI ( $>300$  mL). There were no adverse events related to any of the intravascular modalities after procedure. No pullback repetition was required for IVUS before PCI, whereas  $1.09 \pm 0.29$  pullbacks were needed to properly image the ROI after PCI. FD-OCT required  $1.25 \pm 0.44$  and  $1.29 \pm 0.46$  pullbacks, respectively, for satisfactory pre- and post-PCI assessments. The reasons for repeated pullbacks are summarized in Table III. Matched pre- and post-PCI images were available for analysis in 32 patients, whereas post-PCI images of both IVUS and FD-OCT were available in 34 patients. Twenty-one patients fulfilled the criteria and accepted

TABLE II. Angiographic Characteristics<sup>a</sup>

	Patients (n = 35)
<i>Lesion location</i>	
Ostial only, n (%)	0 (0)
Mid-shaft only, n (%)	1 (2.9)
Distal only, n (%)	22 (62.9)
Ostial and Mid-shaft, n (%)	0 (0)
Mid-shaft and distal, n (%)	11 (31.4)
Ostial and distal, n (%)	1 (2.9)
Ostial mid-shaft distal, n (%)	0 (0)
<i>Medina classification</i>	
(1,1,1), n (%)	7 (20)
(1,1,0), n (%)	9 (25.7)
(1,0,1), n (%)	1 (2.9)
(1,0,0), n (%)	3 (8.6)
(0,1,1), n (%)	5 (14.3)
(0,1,0), n (%)	9 (25.7)
(0,0,1), n (%)	1 (2.9)
<i>QCA</i>	
Nonstented segment	
MLD (mm)	0.96 ± 0.37
RVD (mm)	3.5 ± 0.70
%DS	72.6 ± 8.6
Stented segment	
MLD (mm)	3.14 ± 0.53
RVD (mm)	3.54 ± 0.53
%DS	9.03 ± 4.00
<i>Procedure characteristics</i>	
Strategy	
Single stent, n (%)	27 (77.1)
Two stent, n (%)	6 (17.1)
POBA, n (%)	2 (5.7)
Stent type	
Sirolimus-eluting stents, n (%)	15 (37.5)
Everolimus-eluting stent, n (%)	25 (62.5)
Total number of stents	40
Number of stents per patient	1.14
Average stent diameter	3.4 ± 0.18
Total length of stents (main branch) per patient	24.6 ± 12.4
Patients without ULM ostial stent coverage	6/33 (18.2)

<sup>a</sup>Values are n (%) or mean ± SD.

Abbreviations: QCA: quantitative coronary angiography, MLD: minimum lumen diameter, RVD: reference vessel diameter, DS: diameter stenosis, POBA: plain balloon angioplasty, and ULM: unprotected left main.

repeated angiography and FD-OCT imaging at 1-year follow-up (Fig. 1).

**IVUS and FD-OCT findings.** Left main ostium was properly imaged in only four (12.5%) patients with FD-OCT, and in 31 (93.9%) patients with IVUS ( $P < 0.001$ ) at pre-PCI. Proximal stent edge was imaged in six (18.2%) patients with FD-OCT, and in 30 (90.9%) patients with IVUS ( $P < 0.001$ ); however, when the stent was implanted without ostium coverage ( $n = 6$ ), FD-OCT was able to properly assess proximal stent edge in 100% of the cases (Table IV). The distal segments of the ROI were adequately assessed by both methods in pre- and post-PCI evaluations in almost all cases (Table IV). Visualized lesion length as well as

TABLE III. Imaging Procedures Characteristics<sup>a</sup>

	IVUS	FD-OCT	P-value
<i>PRE-PCI</i>			
Attempted case number, n (%)	35	35	
Unable to cross the catheter, n (%)	2 (5.7)	3 (8.6)	0.317
Successful imaging, n (%)	33/33(100)	31/32(96.9)	0.313
<i>Safety</i>			
ST change	1 (2.9)	1 (2.9)	1.000
Dissection	0 (0.0)	0 (0.0)	NA
Arrhythmia	0 (0.0)	0 (0.0)	NA
Slow flow	0 (0.0)	0 (0.0)	NA
Spasm	0 (0.0)	0 (0.0)	NA
Total number of pullbacks/lesion, mean	1	1.25 ± 0.44	0.003
Patients with repeated pullbacks	0 (0.0)	8 (25.0)	0.004
<i>Reason for repeat pullback</i>			
Insufficient blood clearance	NA	6 (75.0)	NA
Long lesion	NA	2 (25.0)	NA
<i>Volume of contrast</i>			
Total volume of contrast dye/pullback	0	17.8 ± 6.2	NA
Velocity rate	0	4.7 ± 0.56	NA
<i>Post-PCI</i>			
Attempted case number, n (%)	35	35	
Reason for excluding PRE OCT			
Amount of injected contrast, n (%)	0 (0.0)	1 (2.9)	0.317
Successful imaging, n (%)	35/35 (100)	34/34 (100)	NA
<i>Safety</i>			
ST change	0 (0.0)	0 (0.0)	NA
Dissection	0 (0.0)	0 (0.0)	NA
Arrhythmia	0 (0.0)	0 (0.0)	NA
Slow flow	0 (0.0)	0 (0.0)	NA
Spasm	0 (0.0)	0 (0.0)	NA
Total number of pullbacks/lesion, mean	1.09 ± 0.28	1.29 ± 0.46	0.006
Patients with repeated pullbacks	3 (8.6)	10 (29.4)	0.008
<i>Reason for repeat pullback</i>			
Insufficient blood clearance	0 (0.0)	5 (50.0)	0.210
Long lesion	0 (0.0)	2 (20.0)	
Additional balloon angioplasty	2 (66.7)	2 (20.0)	
Additional stent implantation	1 (33.3)	1 (10.0)	
<i>Volume of contrast</i>			
Total volume of contrast dye/pullback	NA	18.7 ± 6.7	NA
Velocity rate	NA	4.9 ± 0.57	NA

<sup>a</sup>Values are n (%) or mean ± SD; NA: not applicable.

stent length was shorter with FD-OCT compared with IVUS ( $20.72 \pm 10.05$  vs.  $21.89 \pm 10.44$  mm,  $P = 0.01$ , and  $22.44 \pm 12.08$  vs.  $23.55 \pm 12.1$  6 mm,  $P = 0.014$ , respectively), mostly as a result of blood contamination at the ostium. Intraluminal thrombus was observed only with FD-OCT (Table IV). Mean lumen and stent areas were similar between FD-OCT and IVUS ( $11.24 \pm 2.66$  vs.  $10.85 \pm 2.47$  mm<sup>2</sup>,  $P = 0.13$  and  $10.44 \pm 2.33$  vs.  $10.49 \pm 2.32$  mm<sup>2</sup>,  $P = 0.82$ , respectively). The limits of agreement for MeanLA are also reported (Fig. 2). FD-OCT detected larger areas and volumes of malapposition when compared to IVUS (Table IV and Fig. 3), as well as more distal edge

dissections. One proximal stent edge dissection identified by FD-OCT was unnoticed by IVUS (Fig. 4). There was one case with incomplete visualization of

the entire vessel (out of screen) pre-PCI, whereas no out-of-screen images were revealed post-PCI (Table IV).

**TABLE IV. IVUS and FD-OCT Imaging Analysis<sup>a</sup>**

	IVUS	FD-OCT	P-value
<b>Pre-PCI</b>			
<i>Lesion completeness</i>			
Proximal completeness, n (%)	31 (93.9)	4 (12.5)	<0.001
Distal completeness, n (%)	33 (100)	29 (90.6)	0.081
Total length (mm)	21.89 ± 10.44	20.72 ± 10.05	0.010
ULM body length (mm)	7.53 ± 3.57	6.45 ± 3.35	0.002
<i>Lumen area (mm<sup>2</sup>)</i>			
Mean	7.58 ± 2.61	7.60 ± 2.63	0.936
Min	3.46 ± 1.66	2.94 ± 1.77	0.002
Intraluminal thrombus, n (%) PRE	0 (0.00)	3 (9.4)	0.081
Vessel out of screen, n (%)	NA	1 (0.1)	NA
<b>Post-PCT</b>			
<i>Stent completeness</i>			
Proximal completeness, n (%)	30/33 (90.9)	6/33 (18.2)	<0.001
Proximal completeness (without ULM ostial stent coverage), n (%)	6/6 (100)	6/6 (100)	NA
Distal completeness, n (%)	33/33 (100)	33/33 (100)	NA
Total stent length (mm)	23.55 ± 12.16	22.44 ± 12.08	0.014
ULM body stent length (mm)	8.26 ± 3.52	7.13 ± 3.60	0.014
<i>Lumen area (mm<sup>2</sup>)</i>			
Mean	10.85 ± 2.47	11.24 ± 2.66	0.132
Min	7.21 ± 2.23	7.18 ± 2.15	0.875
<i>Stent area (mm<sup>2</sup>)</i>			
Mean	10.44 ± 2.33	10.49 ± 2.32	0.821
Min	6.88 ± 2.03	6.79 ± 2.09	0.534
<i>Reference</i>			
Lumen area (mm <sup>2</sup> )	7.81 ± 2.71	7.94 ± 2.37	0.641
Tissue protruding area (mm <sup>2</sup> )	0.11 ± 0.07	0.23 ± 0.09	<0.001
Malapposition area (mm <sup>2</sup> )	0.12 ± 0.36	0.43 ± 0.51	<0.001
Malapposition volume (mm <sup>3</sup> )	1.95 ± 5.69	7.73 ± 7.60	<0.001
Intraluminal thrombus, n (%)	0 (0.00)	2 (5.9)	0.154
Proximal edge dissection, n (%)	0 (0.00)	1 (3.0)	0.317
Distal edge dissection, n (%)	2 (6.1)	10 (30.3)	0.011

<sup>a</sup>Values are n (%) or mean ± SD.

Abbreviations; NA: not applicable and ULM: unprotected left main.

**One-year follow-up FD-OCT imaging.** There were no adverse clinical outcomes associated with repeated FD-OCT imaging of ULM at 1-year follow-up. No cases of CIN were demonstrated. There were no thrombus detected in association with malapposed or uncovered stent struts. Although there was reduction in malapposed stent area when compared to baseline post-procedure images, malapposition was still observed at 1-year follow-up. Postprocedure stent edge dissections were no longer observed at 1-year follow-up (Table V).

**Clinical outcomes.** Two patients developed acute CIN after PCI but recovered to baseline creatinine before hospital discharge. There were no MI, ST, or deaths during the first year post-ULM PCI; however, two patients underwent TLR.

## DISCUSSION

This study provides initial evidence of the safety and feasibility of using FD-OCT to assess, guide, and monitor outcomes of PCI in ULM coronary disease. FD-OCT showed a similar high safety profile compared with IVUS both pre- and post-PCI (Table III). Although FD-OCT was superior in detecting stent malapposition, tissue protrusion, thrombus, and edge dissections, the present data highlight some inherent technical limitations of the technology.

FD-OCT was associated with the use of additional iodine contrast and required more imaging pullbacks than IVUS. The main reasons for pullback repetitions in FD-OCT were lesion length exceeding the default scan length of current FD-OCT system (54 mm/pullback v. 100 mm/pullback in IVUS), and insufficient blood clearance, mainly in the proximal segment of

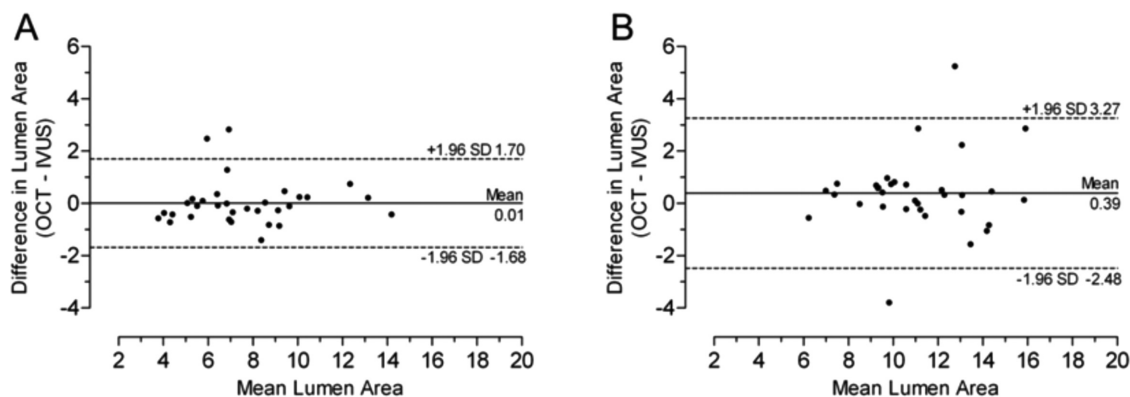


**Fig. 2. Bland-Altman plots for comparison of MeanLA measurements evaluated by FD-OCT and IVUS at pre- (A) and post-PCI (B). IVUS: intravascular ultrasound and FD-OCT: frequency-domain optical coherence tomography.**

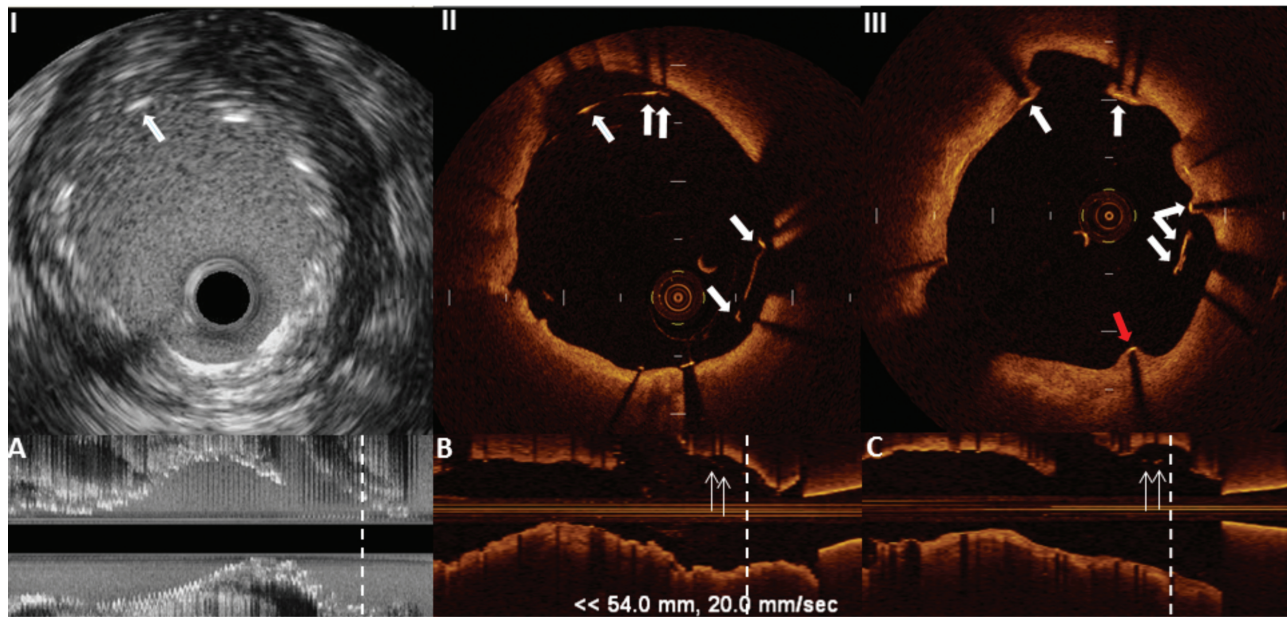


**Fig. 3.** Stent strut malapposition detected by FD-OCT and unrevealed by IVUS. **A** IVUS longitudinal view of a stented segment post-PCI. The region highlighted by the white dashed line is represented in **(I)**; a malapposed stent strut (white arrow) is shown. **(B)** The FD-OCT longitudinal view of the same region demonstrates stent strut malapposition in the proximal segment (white arrows). It is shown in the cross-

section coregistered with IVUS image that FD-OCT is capable of identifying additional malapposed struts **(II, white arrows)**. **(C)** FD-OCT longitudinal view of the same segment at 1-year follow-up highlights malapposed struts (white arrows). The cross-section image corresponding to the white dashed line is represented in **(III)**; persistent (white arrows) and late acquired malapposition (red arrow) are shown.

ULM. To create a virtually blood-free environment to acquire a clear image by FD-OCT [6], blood must be adequately displaced by iodine contrast injection through a well-engaged guiding catheter, which inevitably obscures visualization of the ULM ostium. IVUS offered 1-mm longer visualization of the proximal ULM, and hence, the present data confirm the limitation of current FD-OCT technology to assess disease severity or optimization of stent deployment in ULM ostium.

Several studies have reported the safety and feasibility of non-ULM FD-OCT imaging in the clinical setting [7–9,19,20]. In line with those reports, no concerns regarding ULM FD-OCT assessments were revealed either at baseline post-PCI or at 1-year follow-up in our study. Further confirmation of our results in larger trials is warranted. Differences in imaging technique, number of pullbacks, or lesion length may explain the slight increase in contrast volume (Table III) used in our study compared to some of these reports [9,19]. Nevertheless, the incidence of CIN was lower than those reported previously for PCI without OCT imaging [21]. The two patients with CIN in our study have recovered their baseline renal function. Nevertheless, it remains imperative to take into consideration the total procedural amount of contrast, as well

as other important clinical features such as baseline renal impairment, diabetes mellitus, and hypotension when performing FD-OCT imaging [21].

There were no significant differences in quantitative measurements between IVUS and FD-OCT, except for MLA preprocedure. Whether these differences are owing to overestimation of MLA by IVUS or underestimation by FD-OCT remains to be further investigated. We reported excellent agreements between FD-OCT and IVUS measurements, and high reproducibility of FD-OCT quantification in a phantom model [22]. A possible explanation for the smaller MLA might be the greater resolution of FD-OCT when compared to IVUS, which enables a sharper delineation of luminal borders and less tracing interpolation. FD-OCT's faster pullback as compared to IVUS (20 vs. 1 mm/sec) might have precluded the selection of frames at maximum diastole although one should also observe the differences in reference measurements which did not occur in this study [23]. Importantly, FD-OCT was able to image the entire lumen and stent circumferences in most of cases, which represents a substantial improvement when compared to the previous generation TD-OCT assessments of ULM [24].

IVUS has been available for decades, but its value in ULM PCI was only recently recognized [5]. OCT

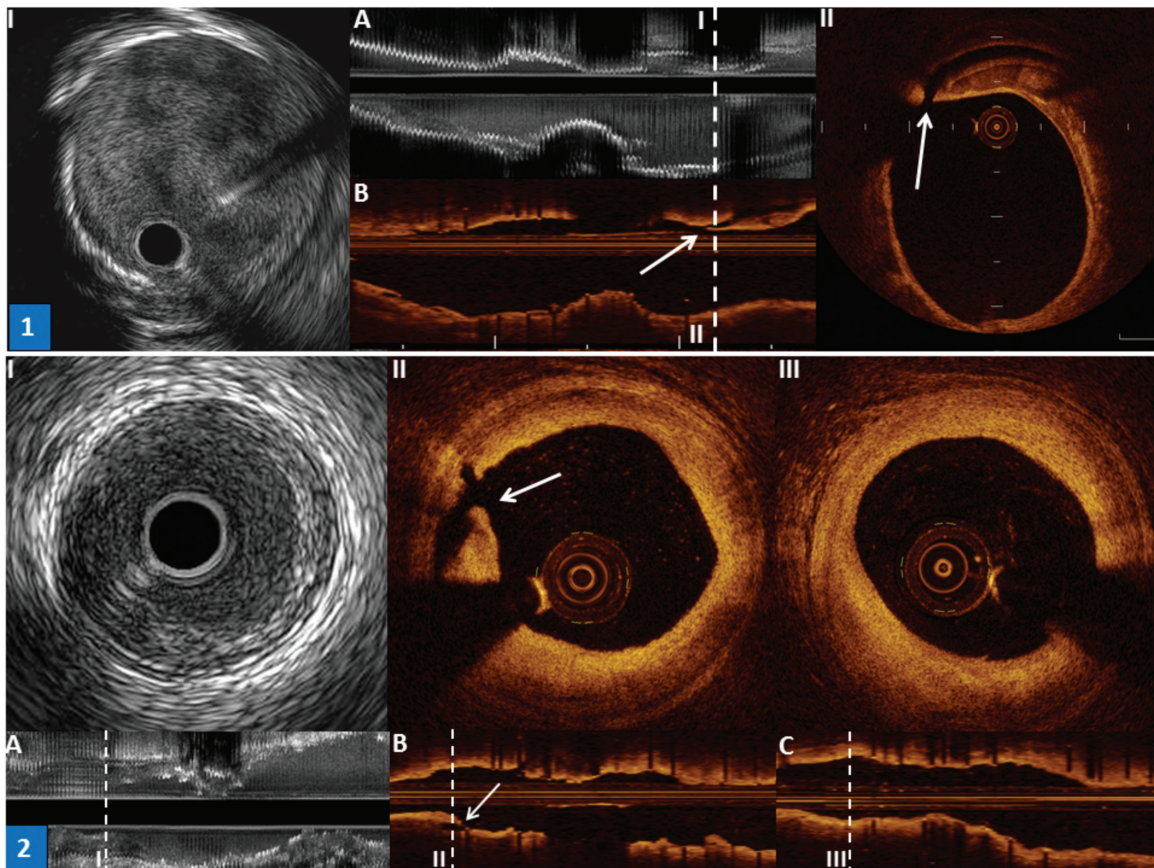


**Fig. 4.** Proximal and distal stent edge dissections identified by FD-OCT and unrevealed by IVUS. Panel 1: (A) An IVUS longitudinal view of a stented segment. The cross-sectional image corresponding to the white dashed line is represented in (I); no pathological findings are demonstrated. FD-OCT longitudinal view of the same region shows a dissection in the distal edge of the stent (B, white arrow). The white dashed line highlights the coregistered spot and the correspondent cross-sectional image (II) demonstrates the edge dissection (white arrow). (C) The same region at 1-year follow-up does not show the dissection anymore. The healing of the dissection is confirmed by the cross-sectional image represented in (III).

**TABLE V.** Post-PCI and Follow-up FD-OCT Imaging Analysis<sup>a</sup>

	FD-OCT (post-PCI)	FD-OCT (follow-up)	<i>P</i> -value
<i>N</i> = 21			
<i>Lumen area</i> (mm <sup>2</sup> )			
Mean	10.83 ± 2.31	9.83 ± 2.18	0.002
Min	7.31 ± 2.16	5.89 ± 2.03	0.001
<i>Stent area</i> (mm <sup>2</sup> )			
Mean	10.22 ± 2.11	10.43 ± 1.92	0.299
Min	6.90 ± 2.15	6.57 ± 2.04	0.317
<i>Tissue protruding area</i> (mm <sup>2</sup> )	0.23 ± 0.12	–	NA
NIH area (mm <sup>2</sup> )	–	0.85 ± 0.55	NA
Malapposition area (mm <sup>2</sup> )	0.27 ± 0.25	0.13 ± 0.14	0.002
Malapposition volume (mm <sup>3</sup> )	5.72 ± 6.31	3.07 ± 3.85	0.027
Intraluminal thrombus, <i>n</i> (%)	0 (0.00)	0 (0.00)	NA
Proximal edge dissection, <i>n</i> (%)	0 (0.00)	0 (0.00)	NA
Distal edge dissection, <i>n</i> (%)	5 (23.8)	0 (0.00)	0.031

<sup>a</sup>Values are *n* (%) or mean ± SD.

Abbreviations: NA: not applicable and NIH: neointimal hyperplasia.

line post-PCI. The cross-sectional image corresponding to the white dashed line is represented in (I); no pathological findings are demonstrated. FD-OCT longitudinal view of the same region shows a dissection in the distal edge of the stent (B, white arrow). The white dashed line highlights the coregistered spot and the correspondent cross-sectional image (II) demonstrates the edge dissection (white arrow). (C) The same region at 1-year follow-up does not show the dissection anymore. The healing of the dissection is confirmed by the cross-sectional image represented in (III).

has been shown to be superior to IVUS to detect malapposition [25], a phenomenon previously associated with ST [26], in nonleft main coronary segments. In our study, FD-OCT visualized significantly more stent strut malapposition than IVUS (Table IV). In addition, distal edge dissections, which have also been linked to adverse outcomes [27], were more often visualized by FD-OCT. Another potential application of FD-OCT imaging in this setting would be monitoring the results of PCI in lesions involving ULM bifurcation (i.e., assessing results of kissing balloon technique, Fig. 5) with three-dimensional FD-OCT reconstruction [28,29]. Whether FD-OCT-guided PCI can optimize acute results and clinical outcomes in ULM bifurcation remains to be determined. IVUS missed two cases of intrastent thrombus and detected less tissue



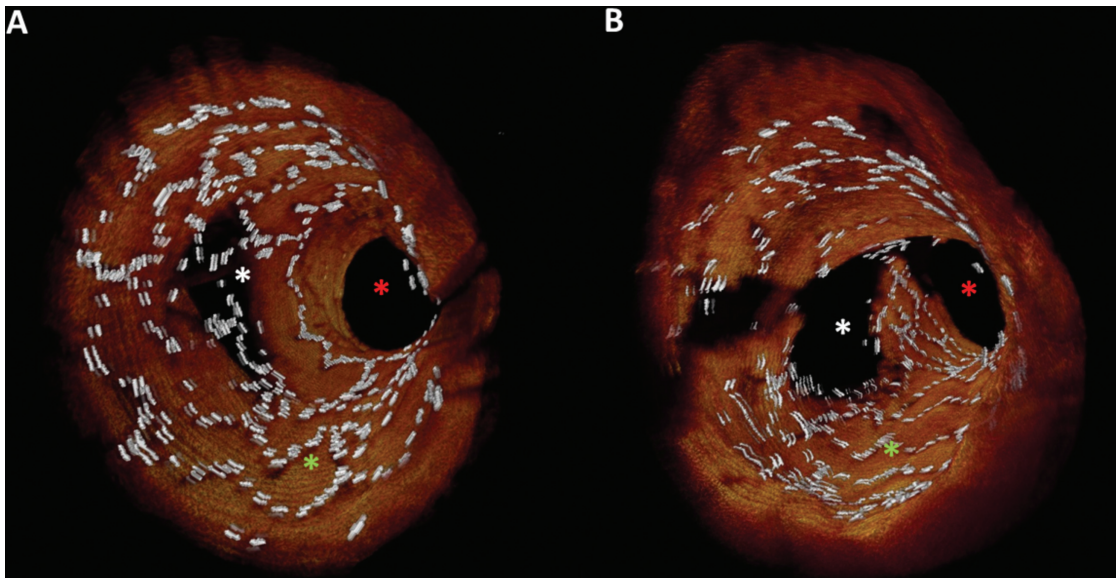


**Fig. 5. Three-dimensional (3D) FD-OCT reconstructions of ULM bifurcation. (A) ULM bifurcation after stent implantation from ULM body to LAD with stent struts jailing LCX ostium, while panel. (B) The same region after kissing balloon technique without stent struts jailing LCX ostium. Green, white, and red asterisks correspond to ULM body, LCX, and LAD, respectively.**

protrusion compared with FD-OCT in our study. Conversely, IVUS was able to assess the majority of ULM ostium (90.9%), whereas FD-OCT enabled ostium assessment in only 18.2% of the cases at post-PCI. Therefore, considering the increasing acceptance of PCI as a treatment strategy for ULM worldwide [30] and the potential catastrophic consequences of ULM complications, the present data support the need for large clinical trials to investigate the impact of different intravascular imaging modalities as well as their potential complementary role to improve patient's outcomes.

This study also demonstrates the safety of performing elective FD-OCT imaging to monitor ULM PCI 1 year after the procedure, supporting the feasibility of utilizing this technology in future ULM clinical trials. Post-PCI edge dissections were healed after 1 year. Although the magnitude of stent malapposition decreased over time [31], this pathological phenomenon was still detected by FD-OCT at 1-year follow-up. The clinical implications of these findings remain unclear and future studies are warranted to determine whether continued dual-antiplatelet therapy beyond the first year should be indicated in patients with persistent, albeit small ULM stent malapposition.

### Study Limitations

The investigators took into consideration the potential risk and futility of dual intravascular imaging during

ULM PCI, which led to a relatively small sample size in this pilot study. Although this report provides the first evidence of the feasibility and safety of FD-OCT in ULM, the study was not designed or powered to evaluate long-term clinical outcomes correlated with FD-OCT findings.

### CONCLUSIONS

In this pilot trial, FD-OCT assessment of ULM was feasible and safe during PCI and at 1-year follow-up. FD-OCT was able to achieve imaging completeness less often compared with IVUS, but it was more sensitive in detecting malapposition and edge dissections. Equivalence between the methods was demonstrated in the assessment of lumen and stent dimensions. Further studies are necessary to investigate the impact of different intravascular imaging modalities as well as their potential complementary role to improve patient's outcomes in ULM PCI.

### Disclosure

Dr. Bezerra has received honoraria from St. Jude Medical, and research grant from Boston Scientific, Abbott, Medtronic. Dr. Costa is on the Speakers' Bureaus of and is a consultant for Daiichi-Sankyo, St. Jude Medical, Inc, Boston Scientific, Sanofi-Aventis, Eli Lilly, and Medtronic; he is also on the Speakers' Bureaus of and is a member of the Scientific Advisory Boards for Abbott, Cordis, St Jude Medical, Inc., and

Scitech. Dr. Attizzani has received consulting fees from St. Jude Medical, Inc.

## REFERENCES

- Mehilli J, Kastrati A, Byrne RA, Bruskina O, Iijima R, Schulz S, Pache J, Seyfarth M, Massberg S, Laugwitz KL, Dirschinger J, Schömig A. Paclitaxel- versus sirolimus-eluting stents for unprotected left main coronary artery disease. *J Am Coll Cardiol* 2009;53:1760–1768.
- Capodanno D, Stone GW, Morice MC, Bass TA, Tamburino C. Percutaneous coronary intervention versus coronary artery bypass graft surgery in left main coronary artery disease a meta-analysis of randomized clinical data. *J Am Coll Cardiol* 2011;58:1426–1432.
- Fitzgerald PJ, Oshima A, Hayase M, Metz JA, Bailey SR, Baim DS, Cleman MW, Deutscher E, Diver DJ, Leon MB, Moses JW, Oesterle SN, Overlie PA, Pepine CJ, Safian RD, Shani J, Simonton CA, Smalling RW, Teirstein PS, Zidar JP, Yeung AC, Kuntz RE, Yock PG. Final results of the can routine ultrasound influence stent expansion (CRUISE) study. *Circulation* 2000;5:523–530.
- Oemrawsingh PV, Mintz GS, Schalij MJ, Zwinderman AH, Jukema JW, van der Wall EE. Intravascular ultrasound guidance improves angiographic and clinical outcome of stent implantation for long coronary artery stenoses: Final results of a randomized comparison with angiographic guidance (TULIP Study). *Circulation* 2003;1:62–67.
- Park SJ, Kim YH, Park DW, Lee SW, Kim WJ, Suh J, Yun SC, Lee CW, Hong MK, Lee JH, Park. Impact of intravascular ultrasound guidance on long-term mortality in stenting for unprotected left main coronary artery stenosis. *Circ Cardiovasc Interv* 2009;2:167–177.
- Bezerra HG, Costa MA, Guagliumi G, Rollins A, Simon DI. Intracoronary optical coherence tomography: A comprehensive review. *J Am Coll Cardiol Interv* 2009;2:1035–1046.
- Stefano G, Bezerra HG, Mehanna E, Yamamoto H, Fujino Y, Wang W, Attizzani G, Chamié D, Simon DI, Costa MA. Unrestricted utilization of frequency domain optical coherence tomography in coronary interventions. *Int J Cardiovasc Imaging*. 2012 Oct 12. [Epub ahead of print].
- Yoon JH, Di Vito L, Moses JW, Fearon WF, Yeung AC, Zhang S, Bezerra HG, Costa MA, Jang IK. Feasibility and safety of the second-generation, frequency domain optical coherence tomography (FD-OCT): A multicenter study. *J Invasive Cardiol* 2012;24:206–209.
- Prati F, Di Vito L, Biondi-Zoccai G, Occhipinti M, La Manna A, Tamburino C, Burzotta F, Trani C, Porto I, Ramazzotti V, Imola F, Manzoli A, Matera L, Cremonesi A, Albertucci M. Angiography alone versus angiography plus optical coherence tomography to guide decision-making during percutaneous coronary intervention: The Centro per la Lotta contro l'Infarto-Optimisation of Percutaneous Coronary Intervention (CLI-OPCI) study. *Eurointervention* 2012;7:823–829.
- Biondi-Zoccai GG, Lotrionte M, Anselmino M, Moretti C, Agostoni P, Testa L, Abbate A, Cosgrave J, Laudito A, Trevisani GP, Sheiban I. Systematic review and meta-analysis of randomized clinical trials appraising the impact of cilostazol after percutaneous coronary intervention. *Am Heart J* 2008;155:1081–1089.
- Van der Zwet PM, Reiber JH. A new approach for the quantification of complex lesion morphology: The gradient field transform; basic principles and validation results. *J Am Coll Cardiol* 1994;24:216–224.
- Mehanna EA, Attizzani GF, Kyono H, Hake M, Bezerra HG. Assessment of coronary stent by optical coherence tomography, methodology and definitions. *Int J Cardiovasc Imaging* 2011;2:259–269.
- Kume T, Akasaka T, Kawamoto T, Ogasawara Y, Watanabe N, Toyota E, Neishi Y, Sukmawan R, Sadahira Y, Yoshida K. Assessment of coronary arterial thrombus by optical coherence tomography. *Am J Cardiol* 2006;97:1713–1717.
- Bouma BE, Tearney GJ, Yabushita H, Shishkov M, Kauffman CR, DeJoseph Gauthier D, MacNeill BD, Houser SL, Aretz HT, Halpern EF, Jang IK. Evaluation of intracoronary stenting by intravascular optical coherence tomography. *Heart* 2003;89:317–320.
- Panse N, Brett S, Panse P, Kareti K, Rewis D, Gilmore P, Zenni MM, Wilke N, Bass T, Costa MA. Multiple plaque morphologies in a single coronary artery: Insights from volumetric intravascular ultrasound. *Catheter Cardiovasc Intervent* 2004;61:376–380.
- Gibson CM, Cannon CP, Daley WL, Dodge JT Jr, Alexander B Jr, Marble SJ, McCabe CH, Raymond L, Fortin T, Poole WK, Braunwald E. TIMI frame count: A quantitative method of assessing coronary artery flow. *Circulation* 1996;93:879–888.
- Harjai KJ, Raizada A, Shenoy C, Sattur S, Orshaw P, Yaeger K, Boura J, Aboufars A, Sporn D, Stapleton D. A comparison of contemporary definitions of contrast nephropathy in patients undergoing percutaneous coronary intervention and a proposal for a novel nephropathy grading system. *Am J Cardiol* 2008;101:812–819.
- Medina A, de Lezo J, Pan M. A new classification of coronary bifurcation lesions. *Rev Esp Cardiol*. 2006;59:183.
- Imola F, Mallus MT, Ramazzotti V, Manzoli A, Pappalardo A, Di Giorgio A, Albertucci M, Prati F. Safety and feasibility of frequency domain optical coherence tomography to guide decision making in percutaneous coronary intervention. *Eurointervention* 2010;6:575–581.
- Takarada S, Imanishi T, Liu Y, Ikejima H, Tsujioka H, Kuroi A, Ishibashi K, Komukai K, Tanimoto T, Ino Y, Kitabata H, Kubo T, Nakamura N, Hirata K, Tanaka A, Mizukoshi M, Akasaka T. Advantage of next-generation frequency-domain optical coherence tomography compared with conventional time-domain system in the assessment of coronary lesion. *Catheter Cardiovasc Interv* 2010;75:202–206.
- ACT Investigators. Acetylcysteine for prevention of renal outcomes in patients undergoing coronary and peripheral vascular angiography: main results from the randomized acetylcysteine for contrast-induced nephropathy trial (ACT). *Circulation* 2011;124:1250–1259.
- Tahara S, Bezerra H, Baibars M, Kyono H, Wang W, Pokras S, Mehanna E, Petersen CL, Costa MA. In vitro validation of new Fourier-domain optical coherence tomography. *Eurointervention* 2011;6:875–882.
- Gonzalo N, Serruys PW, Garcia-Garcia HM, van Soest G, Okamura T, Ligthart J, Knaapen M, Verheye S, Bruining N, Regar E. Quantitative ex vivo and in vivo comparison of lumen dimensions measured by optical coherence tomography and intravascular ultrasound in human coronary arteries. *Rev Esp Cardiol* 2009;62:615–624.
- Parodi G, Maehara A, Giuliani G, Kubo T, Mintz GS, Migliorini A, Valenti R, Carrabba N, Antoniucci D. Optical coherence tomography in unprotected left main coronary artery stenting. *Eurointervention* 2010;6:94–99.
- Ozaki Y, Okamura M, Ismail T, Naruse H, Hattori K, Kan S, Ishikawa M, Kawai T, Takagi Y, Ishii J, Prati F, Serruys PW. The fate of incomplete stent apposition with drug-eluting stents:

- An optical coherence tomography-based natural history study. *Eur Heart J* 2010;31:1470–1476.
26. Hassan AK, Berghuan SC, Stijen T, van der Hoeven BL, Snoep JD, Plevier JW, Schali J, WouterJukema J. Late stent malapposition risk is higher after drug-eluting stent compared with bare-metal stent implantation and associates with late stent thrombosis. *Eur Heart J* 2010;31:1172–1180.
  27. Choi SY, Witzendichler B, Maehara A, Lansky AJ, Guagliumi G, Brodie B, Kellett MA Jr, Dressler O, Parise H, Mehran R, Dangas GD, Mintz GS, Stone GW. Intravascular ultrasound findings of early stent thrombosis after primary percutaneous intervention in acute myocardial infarction: A harmonizing outcomes with revascularization and stents in acute myocardial infarction (HORIZONS-AMI) substudy. *Circ Cardiovasc Intervent* 2011;4:239–247.
  28. Farooq V, Serruys PW, Heo JH, Gogas BD, Okamura T, Gomez-Lara J, Brugaletta S, Garcia-Garcia HM, van Geuns RJ. New insights into the coronary artery bifurcation hypothesis-generating concepts utilizing 3-dimensional optical frequency domain imaging. *J Am Coll Cardiol Intervent* 2011;4:921–931.
  29. Alegría-Barrero E, Foin N, Chan PH, Syrseloudis D, Lindsay AC, Dimopolous K, Alonso-González R, Viceconte N, De Silva R, Di Mario C. Optical coherence tomography for guidance of distal cell recrossing in bifurcation stenting: Choosing the right cell matters. *EuroIntervention* 2012;8:205–213.
  30. Levine GN, Bates ER, Blankenship JC, Bailey SR, Bittl JA, Cercek B, Chambers CE, Ellis SG, Guyton RA, Hollenberg SM, Khot UN, Lange RA, Mauri L, Mehran R, Moussa ID, Mukherjee D, Nallamothu BK, Ting HH. 2011 ACCF/AHA/SCAI Guideline for percutaneous coronary intervention: Executive summary: A report of the American College of Cardiology Foundation/American Heart Association task force on practice guidelines and the Society for Cardiovascular Angiography and Interventions. *Circulation* 2011;124:2574–2609.
  31. Guagliumi G, Bezerra HG, Sirbu V, Ikejima H, Musumeci G, Biondi-Zoccai G, Lortkipanidze N, Fiocca L, Capodanno D, Wang W, Tahara S, Vassileva A, Matiashvili A, Valsecchi O, Costa MA. Serial assessment of coronary artery response to paclitaxel-eluting stents using optical coherence tomography. *Circ Cardiovasc Intervent* 2012;5:30–8.